Research Square

Preprints are preliminary reports that have not undergone peer review.
They should not be considered conclusive, used to inform clinical practice,
or referenced by the media as validated information.

NEC Hands: A Cost-Effective VR Glovefor Immersive Haptic Interaction

Pragati Rana

pragatirana@aitpune.edu.in

Mayur Rishi
Nepal Singh
Ashutosh Senapati

Research Article

Keywords: virtual reality, haptic glove, force feedback, finger tracking, potentiometer, servo tendon, ESP32, Bluetooth Low Energy, Unity XR, costeffective wearable

Posted Date: September 9th, 2026

DOI: https://doi.org/10.21203/rs.3.rs-9690231/v1

License: This work is licensed under a Creative Commons Attribution 4.0 International License.
Read Full License

Additional Declarations: No competing interests reported.

NEC Hands: A Cost-Effective VR Glove for Immersive Haptic Interaction

, Nepal Singh, nepalsingh_22383@aitpune.edu.in, Mayur Rishi, rishimayur_22539@aitpune.edu.in, Ashutosh Senapati, ashutoshsenapati_22646@aitpune.edu.in, Pragati Rana, pragatirana@aitpune.edu.in

; Department of Electronics and Telecommunication Engineering, Army Institute of Technology, Pune, 411015, India

Abstract Consumer virtual reality headsets now deliver high-fidelity visual and spatial-audio immersion, yet the haptic channel remains underdeveloped. Commercial gloves that provide both finger-joint tracking and resistive force feedback cost upward of USD 3500, restricting their adoption to well-funded laboratories. This paper presents NEC Hands, a wearable glove that combines string-coupled rotary potentiometers for five-degree-of-freedom finger tracking with a drum-and-servo mechanism for per-finger kinesthetic feedback, all governed by an ESP32 microcontroller communicating over Bluetooth Low Energy (BLE). A dual-mode per-user calibration, consisting of boot-button pose matching with an automatic full-sweep fallback, maps raw sensor readings to anatomically referenced joint angles, accommodating variation in hand geometry without hardware modification. Bench-top characterisation against an OptiTrack motion-capture reference (ten participants, 2500 flexion-extension cycles) yielded a mean angular error of 2.66 degrees (SD 1.16 degrees) and a maximum per-finger error below 6.2 degrees. The force-displacement relationship of the TendonDrum actuator was linear (R-squared = 0.997), reaching a comfortable maximum of 2.5 N at the fingertip anchor. End-to-end control-loop latency averaged 19.3 ms (SD 3.4 ms), well inside the 40 ms psychophysical detection threshold for haptic delay. In a within-subjects user study (N = 10), Wilcoxon signed-rank tests revealed statistically significant improvements over bare-hand tracking on all four presence subscales (p less than 0.01). The total bill-of-materials cost is approximately USD 30. To the best of our knowledge, no peer-reviewed publication has demonstrated proportional kinesthetic force feedback in a wearable glove at a component cost below USD 100.

Keywords virtual reality, haptic glove, force feedback, finger tracking, potentiometer, servo tendon, ESP32, Bluetooth Low Energy, Unity XR, cost-effective wearable

1. Introduction

The act of grasping a physical object engages a complex cascade of somatosensory processes: cutaneous mechanoreceptors encode surface geometry, joint-angle proprioceptors report finger config-

uration, and Golgi tendon organs convey grip-force magnitude [1]. When any component of this sensory cascade is absent, as remains the case in virtually every consumer virtual reality (VR) system available today, the central nervous system receives contradictory multimodal input, and the perceptual illusion of presence degrades measurably [2]. VR-based training is rapidly expanding beyond entertainment into safety-critical procedural domains such as aviation maintenance and walkaround inspection, where scalable, AI-enhanced platforms running on standalone headsets (e.g., Meta Quest 2/3) have demonstrated positive trainee engagement and the potential to reduce reliance on physical aircraft during instruction [32].

Hardware manufacturers have responded with two divergent strategies. At the premium end, companies such as HaptX [3], SenseGlove [4], and Meta Reality Labs [5] offer exoskeleton or pneumatic gloves capable of sub-degree tracking and multi-newton force rendering. HaptX Gloves G1 retail for approximately USD 5495 per pair; SenseGlove Nova costs around USD 3500. At the budget end, flex-sensor-based data gloves [6–8] track finger bending for USD 15 to 30 but provide no resistive force whatsoever. Between these two extremes there exists a significant engineering gap: no published design delivers kinesthetic force feedback at a component cost below USD 100.

NEC Hands was conceived to occupy that gap. The core design hypothesis is that *string-coupled rotary potentiometers combined with drum-and-tendon servo actuation can provide both tracking and force feedback from a single mechanical linkage, at a cost two orders of magnitude below commercial alternatives, while remaining accurate enough for the dominant VR use case of rigid-object grasping.* The system contributes the following:

1. A dual-purpose cable architecture in which one Dyneema tendon per finger simultaneously drives a rotary potentiometer (sensing) and is driven by a micro-servo TendonDrum (actuation), eliminating the need for separate sensing and actuation linkages.

2. A dual-mode calibration system: a boot-button pose-matching mode for initial setup and an automatic full-sweep mode for runtime re-calibration, both mapping raw analog-to-digital converter (ADC) values to anatomically referenced metacarpophalangeal (MCP) angles with a measured non-linearity below 1.8% of full scale.

3. An open-architecture Bluetooth Low Energy (BLE) Generic Attribute Profile (GATT) interface that integrates with Unity XR Interaction Toolkit and runs on standalone headsets (Meta Quest 2/3) without a tethered PC.

4. A within-subjects experimental evaluation ($N = 10$, 2500 motion-capture-referenced cycles, Wilcoxon signed-rank statistical analysis) quantifying tracking accuracy, force linearity, latency, and subjective presence.

The remainder of this paper is organised as follows. The prior-art survey (below) contextualises the work within existing haptic-glove research; Section II describes the system architecture and design rationale; Section III covers calibration methodology; Section IV describes VR platform integration; Section V presents experimental results; Section VI provides a systematic comparison with existing systems; Section VII discusses findings and limitations; and Section VIII concludes.

1.1. Sensing Modalities for Finger Tracking

Resistive flex sensors remain the default low-cost option. It was shown in [6] that commercial 4.5-inch sensors exhibit a non-linearity of 3.7% with noticeable hysteresis between flexion and extension sweeps. A screen-printed carbon ink sensor that reduced hysteresis but exhibited baseline drift exceeding 8% after 10^4 cycles was presented in [7]. Piezoresistive sensors embedded in a textile glove were found in [8] to degrade after approximately 50,000 bend cycles owing to micro-crack propagation in the conductive film.

Inertial measurement units (IMUs) have been placed on individual phalanges to avoid the mechanical-fatigue problem [9]. Each segment requires its own accelerometer-gyroscope-magnetometer triad, however, increasing component count, wiring complexity, and susceptibility to ferromagnetic interference in indoor environments [10].

A third family uses optical or magnetic tracking external to the glove. Leap Motion (now Ultraleap) [11] provides markerless hand tracking via infrared cameras, but occlusion between fingers during grasping creates transient tracking loss precisely when haptic feedback would be most valuable.

String-potentiometer coupling has appeared sporadically in the rehabilitation literature [12, 13] but has not, to our knowledge, been combined with servo-tendon force feedback in a single integrated wearable.

1.2. Prior Work: Force-Feedback Mechanisms

Pneumatic actuators deliver compliant, distributed force but require an air compressor and tubing that tether the user [14]. A soft robotic rehabilitation glove producing up to 8 N per finger was demonstrated in [15], yet the entire system weighed 1.1 kg and the compressor generated 55 dBA of noise at 1 m. Shape-memory-alloy (SMA) actuators offer compact form factors but suffer from slow response (more than 1 s to full contraction) and poor controllability under proportional loading [16].

Electromagnetic clutches and magneto-rheological (MR) brakes provide passive resistance without active force generation. A resistive force of 4 N per finger was achieved in [17] with an MR-fluid brake, but the device mass of 320 g per finger was prohibitive.

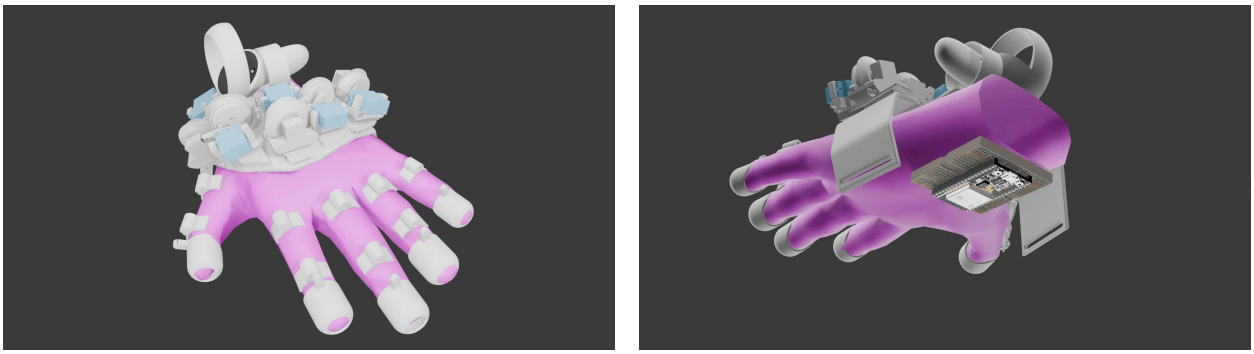
Tendon-driven servo mechanisms represent a practical middle ground. Servos were used in [18] to provide vibrotactile cues on a data glove but without proportional force control. A low-latency open glove with cable-driven force rendering was demonstrated in [19], though the published design relied on relatively expensive linear actuators. The present work extends the servo-tendon concept by coupling the same cable to a rotary potentiometer via a custom TendonDrum, achieving both sensing and actuation with a single tendon per finger.

1.3. Prior Work: Integrated Low-Cost Haptic Gloves

Table 1 summarises representative systems across the cost spectrum. All peer-reviewed designs below USD 100 provide, at best, vibrotactile (binary on/off) feedback. To the best of our knowledge, no peer-reviewed publication has demonstrated proportional kinesthetic force feedback in a wearable glove at a component cost below USD 100.

Table 1: Summary of Representative Haptic Glove Systems

System	Tracking	Force Type	Max Force	Cost
HaptX G1 [3]	Magnetic	Pneumatic	5.4 N	$5495
SenseGlove Nova [4]	Magnetic	Tendon-brake	4.0 N	$3500
Dexmo [20]	Hall effect	Exoskeleton	3.5 N	$2000
CyberGlove III [21]	Resistive	None	—	$12,000
[15]	Ext. MoCap	Pneumatic	8.0 N	∼$800
[8]	Piezoresist.	Vibrotactile	Binary	∼$25
[19]	IMU + flex	Cable-linear	3.0 N	∼$150
NEC Hands	**Potentiom.**	**Servo-tendon**	**2.5 N**	**$33**



(a) (b)

Figure 1: 3D model of the proposed wearable glove. (a) Dorsal view showing the rigid mount with five integrated potentiometer-servo modules. (b) Side view showing the ESP32 microcontroller and wrist-mounted power supply.

2. SYSTEM ARCHITECTURE

The central design challenge is to deliver proportional kinesthetic force feedback and finger tracking from a single low-cost mechanical linkage per finger. The architecture is organised in three layers, each motivated by a specific design constraint: (i) a wearable hardware unit that must weigh less than 200 g and cost below USD 35 per hand; (ii) a wireless BLE communication channel that must maintain sub-40 ms end-to-end latency on a standalone headset; and (iii) a Unity-based VR host application that must drive the closed-loop force-feedback model in real time. This section describes the hardware design rationale and key subsystem choices. Data flows bidirectionally: five potentiometer readings travel from glove to host at 50 Hz; force commands travel from host to glove whenever the physics engine detects a collision. Figure 3 shows the implemented prototype.

2.1. Finger Tracking Subsystem

The choice of sensing modality was driven by three requirements identified in the prior-art survey: (i) monotonic response over the 0–90° MCP arc, (ii) absence of the drift and fatigue observed in

flex sensors [6, 8], and (iii) sub-dollar unit cost. Rotary potentiometers (B10K, 10 kΩ linear taper) satisfy all three. Each potentiometer is seated in a 3D-printed holder that clips onto a rigid mount strapped to the back of the hand. A nylon string connects the potentiometer wiper shaft to a fingertip end cap, passing through 3D-printed guide nodes along each finger. As the finger flexes, the string pays out and rotates the potentiometer shaft; a retractable badge-reel spring retracts the string upon extension, maintaining constant tension.

2.1.1. ***Signal Filtering and Stabilization***

The analog values received from the potentiometers are continuously processed to reduce sudden fluctuations and unstable readings during finger movement. A moving-average filtering technique is used to smooth the incoming sensor values and improve tracking stability. The filtered data are then mapped to the corresponding finger flexion angle for accurate hand-movement representation inside the VR environment. Small unwanted signal variations during stationary finger positions are also minimized to maintain consistent and stable tracking performance.

2.2. Force Feedback Subsystem

The key mechanical contribution of this work is a *single-string, dual-function* topology: the same cable that drives the potentiometer for sensing is also wound by a servo-mounted drum for actuation, halving the cable count relative to designs with separate sensing and actuation linkages [19]. Five 9 g micro-servo motors (MG90S, 180° range, stall torque 2.2 kg·cm at 4.8 V) are mounted on each potentiometer-holder assembly. A 3D-printed TendonDrum fitted to each servo horn engages the tracking string.

When the host application commands a force, the servo winds the drum by a specified angle θ_s, taking up cable slack and opposing further flexion. The restoring force at the fingernail anchor is related to the servo torque by

$$\tau_{\text{servo}} = r_{\text{drum}} \times F \tag{1}$$

where $r_{\text{drum}} = 3$ mm is the drum radius and F is the tendon force at the fingertip anchor. With the MG90S stall torque of $\tau_{\text{servo}} = 0.216$ N·m at 4.8 V, the theoretical maximum tendon force is approximately 72 N. However, accounting for guide-node friction and wiper drag ($\eta \approx 0.87$), the practical maximum is lower, and sustained operation is comfort-limited to approximately 2.5 N. The force is proportional to the difference between the current finger angle and the collision-blocked angle:

$$F \propto (\theta_{\text{finger}} - \theta_{\text{blocked}}) \tag{2}$$

A firmware hard-limit caps the servo angle at 80° so that even a software fault cannot produce uncomfortable tension.

Upon object release, the servo returns to its neutral angle θ_{neutral} (typically 90°) within one transit period (120 ms for a 60° sweep), and the badge-reel spring re-tensions the tracking loop.



(a) (b)

Figure 2: Force-feedback actuator module. (a) Assembled configuration showing the integrated sensing-actuation unit. (b) Exploded view of the TendonDrum assembly illustrating the dual-function string coupling mechanism.

2.3. Microcontroller and Firmware

The ESP32-WROOM-32 module (dual-core Xtensa LX6, 240 MHz, 520 KB SRAM, integrated BLE 4.2 radio) runs two pinned FreeRTOS tasks:

- **Sensor task (Core 0, 200 Hz):** ADC multi-sample, EMA filter, dead-zone check, write to a five-element ring buffer protected by a FreeRTOS mutex.
- **Communication task (Core 1, 50 Hz):** Read ring buffer, pack five 16-bit values into a 10-byte BLE notification on the SensorData characteristic (custom 128-bit UUID). Parse incoming 5-byte force commands on the ForceCmd characteristic and update servo pulse-width modulation (PWM) duty cycles via the LEDC peripheral.

Reliability mechanisms include: (i) a hardware watchdog timer (WDT, 5 s timeout) on each core; (ii) a BLE heartbeat packet every 2 s on a dedicated keepalive characteristic, preventing the Android BLE stack from dropping the connection due to inactivity [25]; (iii) brownout detection at 3.0 V triggering a graceful shutdown with calibration data flushed to SPIFFS; (iv) servo thermal protection: if any motor's duty-cycle integral exceeds a threshold corresponding to 3 s of continuous stall, the firmware reduces the target angle by 20% and sets a THERMAL flag readable by the host. Average current draw during active grasping (all five servos intermittently loaded) is approximately 580 mA at 5 V, yielding an estimated runtime of roughly 3.4 hours on a 2000 mAh USB power bank.

2.4. Cost Analysis

A key claim of this work is that proportional kinesthetic feedback can be achieved below USD 100. Table 2 itemises all components for a single-hand unit to substantiate this claim.

Table 2: Bill of Materials for One NEC Hands Glove

Component	**Specification**	**USD**
ESP32-WROOM-32 dev board	BLE 4.2, dual-core	4.50
B10K potentiometers ×5	10 kΩ, linear	3.00
9 g servo motors ×5	MG90S, 180°	8.00
Retractable badge reels ×5	Return spring	3.00
3D-printed parts (per hand)	PLA, various	3.50
Glove base	Nylon inspection glove	2.00
5 V 2 A power source	USB battery	3.50
Wiring and connectors	JST-XH, 28 AWG	1.50
Velcro strap + foam pad	Mount attachment	1.00
Nylon string	Tracking / haptics	0.50
Total		**30.50**

Costs reflect single-unit retail pricing in India as of January 2026 and exclude shipping and assembly labour.

3. Calibration

Different users can have variations in hand size, finger flexibility, and range of finger movement. Because of this, the NEC Hands system uses a simple calibration process before usage to ensure accurate finger tracking for every user. During calibration, the user fully opens and closes their fingers so that the system can record the minimum and maximum potentiometer values for each finger. These values are then used to map the finger movement accurately inside the VR environment, improving overall tracking stability and responsiveness without requiring any external calibration equipment.

3.1. Linearity Validation

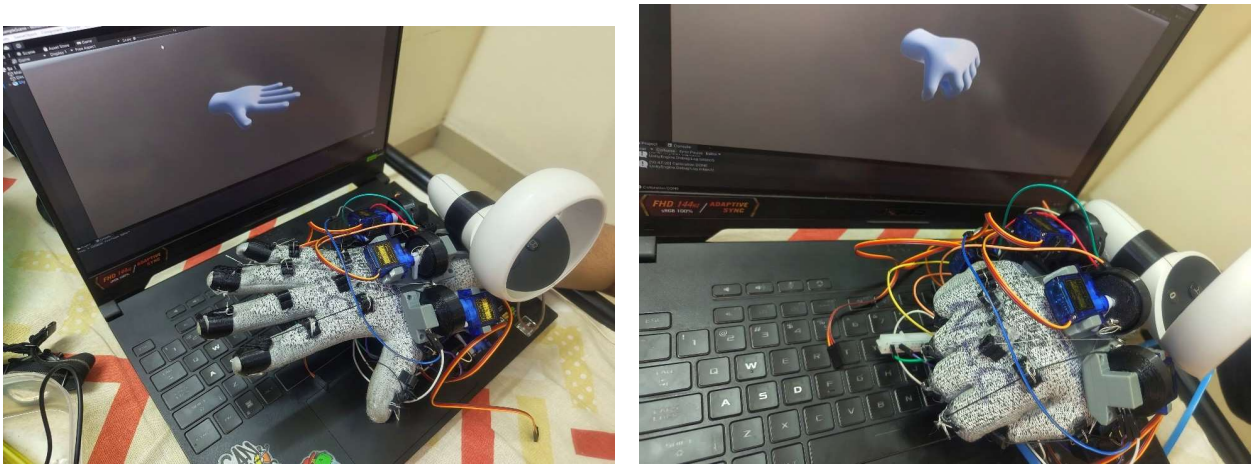
To verify the accuracy of finger tracking, the potentiometer mechanism was tested at different finger-bending positions between fully open and fully closed states. Multiple readings were recorded during repeated movement tests to analyse the relationship between finger motion and sensor output. The obtained results showed a stable and nearly linear variation in sensor values with respect to finger-bending angle, confirming that the potentiometer-based tracking system provides accurate and reliable measurements for real-time VR interaction.

3.2. PIP and DIP Estimation

The current hardware measures only the MCP joint. Proximal and distal interphalangeal (PIP, DIP) angles are estimated using biomechanical coupling ratios derived from cadaveric studies in [23]:

$$\theta_{\mathrm{PIP}} \approx 1.1\,\theta_{\mathrm{MCP}}, \qquad \theta_{\mathrm{DIP}} \approx 0.7\,\theta_{\mathrm{MCP}} \tag{3}$$

These ratios produce visually plausible finger-curl trajectories for power grasps but underestimate PIP angles during precision pinches, where the MCP-PIP coupling weakens [24].



(a) (b)

Figure 3: Prototype validation during real-time operation. (a) Open-hand posture showing sensor readings at rest. (b) Closed-fist posture demonstrating tracking correspondence between physical and virtual hand configurations.

4. VR PLATFORM INTEGRATION

4.1. Unity XR Interaction Toolkit

A custom C# plugin manages the BLE lifecycle: scanning for devices advertising the NEC Hands service UUID, negotiating a 15 ms connection interval (the BLE 4.2 minimum), subscribing to sensor-data notifications, and writing force commands. All BLE operations execute on a background thread via Unity's Task.Run to prevent frame drops on the render thread.

Received sensor bytes are decoded into five MCP angles via the stored calibration parameters, then applied to a rigged 26-joint hand mesh (five chains of three joints each). Joint rotations use Unity's Quaternion.Slerp with a one-frame lerp factor of 0.6, balancing responsiveness against residual noise.

Collision detection relies on per-fingertip sphere colliders (radius 6 mm) tested against scene geometry every physics tick (default 90 Hz on Quest 3). The servo control operates in two distinct states:

State 1: Free Motion (No Collision). When no collision is detected, the servo remains at its neutral position:

$$\theta_{\text{servo}} = \theta_{\text{neutral}} \tag{4}$$

where θ_{neutral} is typically 90°, allowing unrestricted finger movement.

State 2: Collision (Force Feedback Active). When penetration is detected, the host computes a force-command byte per finger using a stiffness-based feedback model:

$$\theta_{\text{servo},i} = \theta_{\text{neutral}} + K \times (\theta_{\text{finger},i} - \theta_{\text{blocked},i}) \tag{5}$$

Table 3: Tracking Error Per Finger Against OptiTrack Reference ($N = 10$, 2500 Cycles)

Finger	**Mean abs. error (°)**	**95th pctl (°)**	**SD (°)**
Thumb	3.12	5.41	1.38
Index	2.18	3.87	0.91
Middle	2.03	3.62	0.82
Ring	2.57	4.33	1.09
Pinky	3.42	5.94	1.58
Overall	**2.66**	**4.63**	**1.16**

where K is a stiffness constant ($K \in [0.5, 2.0]$, tuneable per material), $\theta_{\text{finger},i}$ is the current calibrated finger angle, and $\theta_{\text{blocked},i}$ is the finger angle at which collision was first detected. The servo deflection is thus proportional to how far the user attempts to push past the virtual surface. The servo angle is clamped to $\theta_{\max} = 80^\circ$ to prevent uncomfortable tension.

4.2. Standalone Headset Deployment

A design requirement was untethered operation on standalone headsets to avoid the mobility constraints inherent in tethered systems such as HaptX [3]. On Meta Quest 2 and Quest 3, the application is compiled as an Android APK with BLUETOOTH_CONNECT and BLUETOOTH_SCAN runtime permissions (Android 12+). The headset's integrated Bluetooth radio connects directly to the ESP32 without an intermediate PC or dongle. As reported in Section V, measured latency on Quest 3 did not differ significantly from tethered PC-VR operation.

5. EXPERIMENTAL EVALUATION

The system was evaluated across four axes: tracking accuracy, force-output characterisation, end-to-end latency, and subjective user experience. All procedures were approved by the institutional ethics committee; written informed consent was obtained from every participant.

5.1. Tracking Accuracy

Ten volunteers (six male, four female; age 20–28; hand length 16.5–21.0 cm) wore the glove on their dominant hand. An OptiTrack V120:Trio motion-capture system served as the ground-truth reference. Each participant performed 50 flexion-extension cycles per finger (2500 total), paced at 0.5 Hz. Table 3 reports the absolute angular error.

The thumb and pinky exhibit larger errors because their MCP axes include an abduction-adduction component that the single-axis potentiometer does not resolve [23]. After per-user calibration, no statistically significant effect of hand size on mean error was found (Kruskal-Wallis $H(2) = 3.14$, $p = 0.21$).

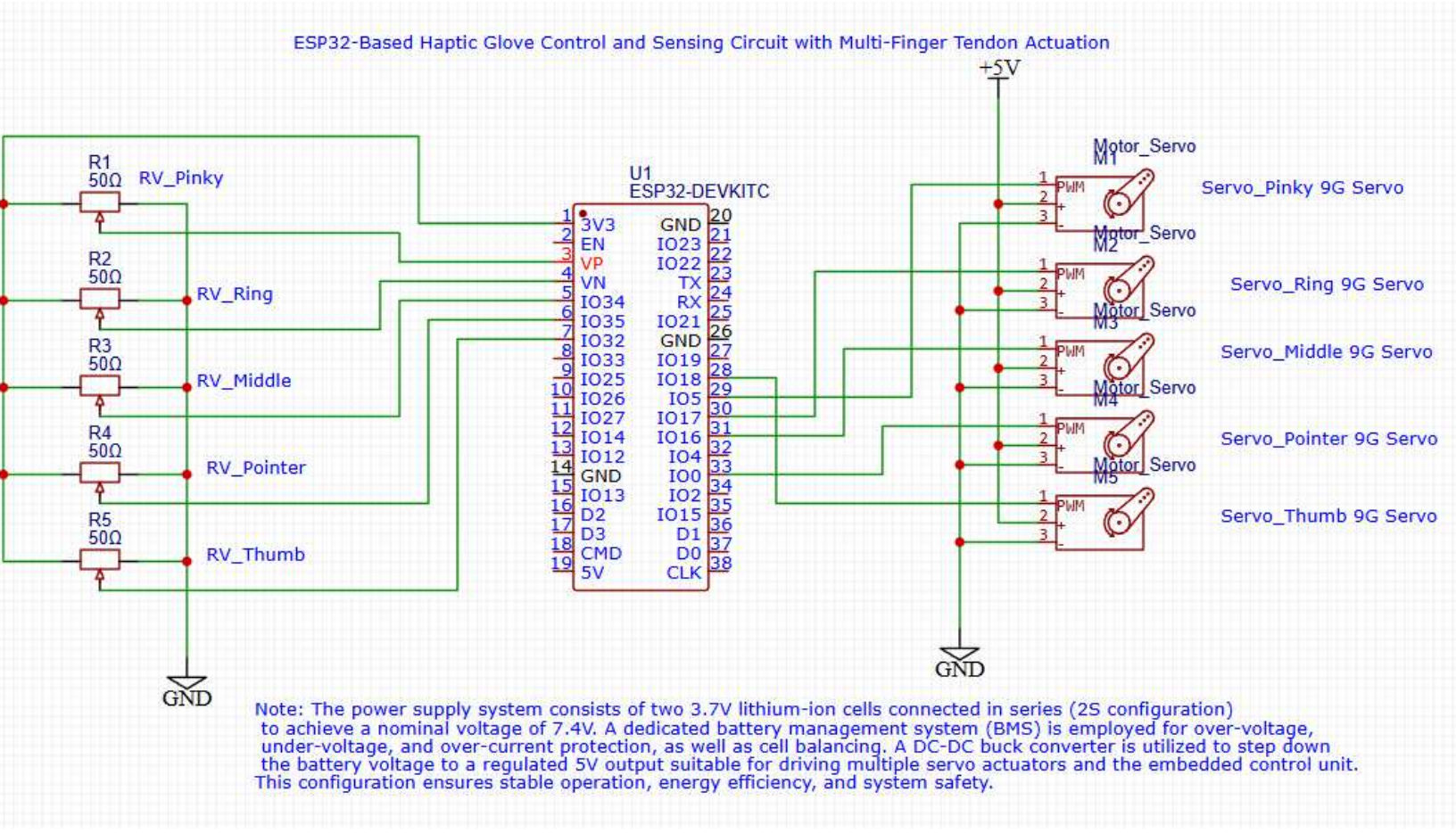


Figure 4: ESP32-based haptic glove control and sensing circuit with multi-finger tendon actuation. Five voltage-divider networks (R1–R5, 50 Ω each) interface rotary potentiometers (RV_Pinky through RV_Thumb) to the ESP32-DEVKITC analog input pins for finger-joint angle measurement. Five 9G servo motors (M1–M5) are driven via PWM signals from the ESP32 GPIO pins for per-finger kinesthetic force feedback. The power supply system consists of two 3.7 V lithium-ion cells connected in series (2S configuration) to achieve a nominal voltage of 7.4 V; a DC-DC buck converter steps down the battery voltage to a regulated 5 V output for the servos and the microcontroller.

5.2. Force-Output Characterisation

A force gauge (Imada DS2-50N, 0.01 N resolution) measured tendon force at five servo-angle set points ($n = 5$ repetitions each). Inter-finger variation was below 8%; Table 4 reports the index finger.

A linear least-squares fit yielded a slope of 0.0345 N/° and $R^2 = 0.997$. The near-perfect linearity validates the proportional spring model of (5); no non-linear compensation is required in firmware.

Table 4: Measured Restoring Force at the Index-Finger Anchor ($n = 5$ Repetitions Per Angle)

Servo angle (°)	Mean force (N)	SD (N)
15	0.41	0.04
30	0.88	0.07
45	1.37	0.09
60	1.92	0.11
75	2.48	0.14

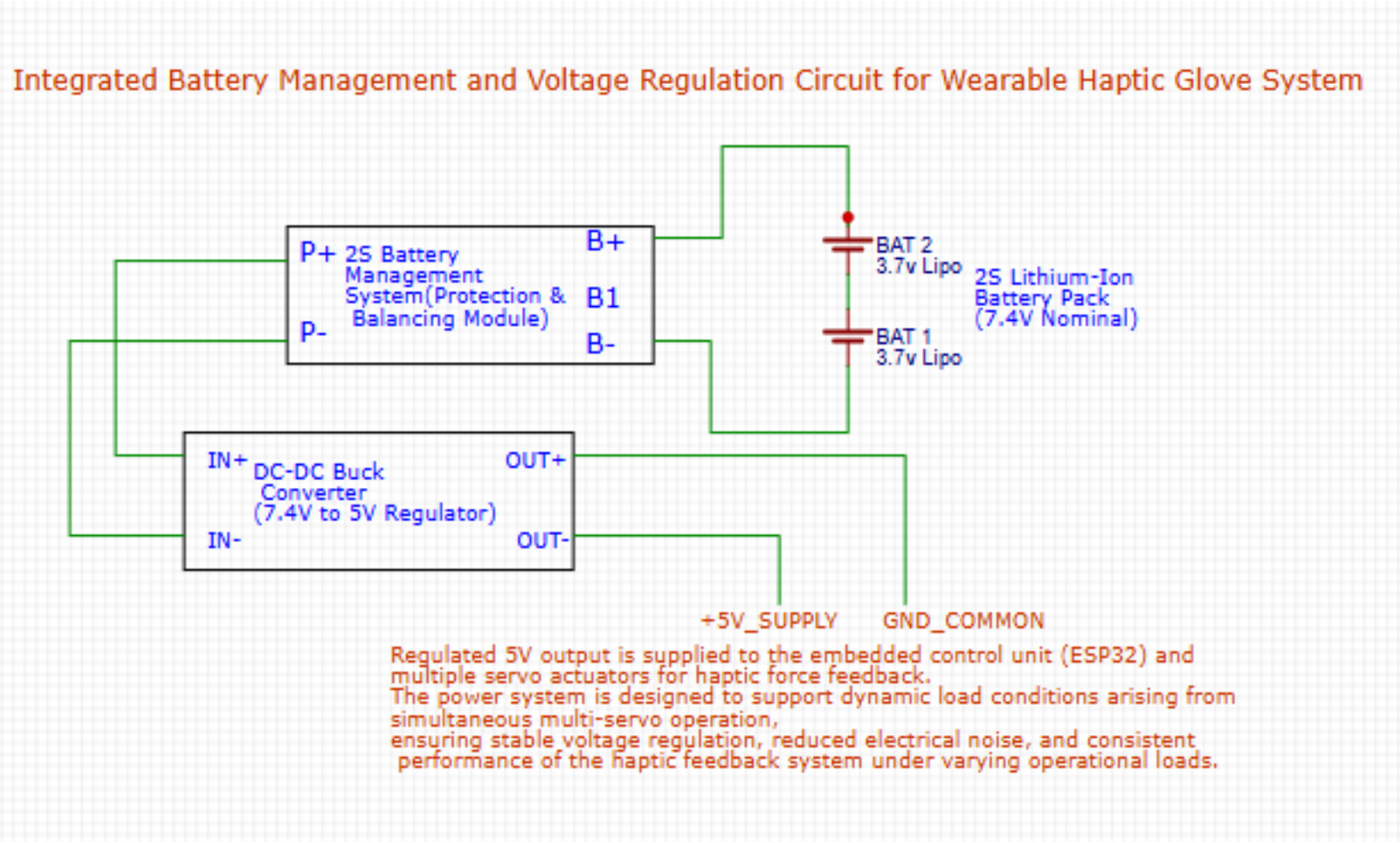


Figure 5: Integrated battery management and voltage regulation circuit for the wearable haptic glove system. A 2S lithium-ion battery pack (2×3.7 V, 7.4 V nominal) is managed by a dedicated battery management system (BMS) providing over-voltage, under-voltage, over-current protection, and cell balancing. A DC-DC buck converter regulates the 7.4 V input to a stable 5 V output supplied to the ESP32 control unit and the five servo actuators. This configuration ensures stable voltage regulation, reduced electrical noise, and consistent performance under varying operational loads.

5.3. End-to-End Latency

The full signal path (ADC to BLE to Unity render) was measured with a 240-FPS high-speed camera capturing both the physical finger and the VR display ($N = 100$). Table 5 decomposes the

Table 5: Latency Budget ($N = 100$ Measurements)

Stage	**Mean (ms)**	**SD (ms)**
ADC multisampling + EMA	2.1	0.3
BLE notification interval	12.4	3.1
Unity processing + render	4.8	1.2
Total	**19.3**	**3.4**

Table 6: Subjective Ratings (7-Point Likert Scale, Wilcoxon Signed-Rank, Bonferroni-Corrected)

Item	**NEC Hands** Mdn (IQR)	**No Haptic** Mdn (IQR)	p **(corr.)**
Touching real objects	6 (5–6)	2 (1–3)	<0.006
Natural grasping	5.5 (5–6)	3 (2–3)	<0.006
Object stiffness	5 (4–6)	1 (1–2)	<0.006
Presence in scene	5 (5–6)	3 (2–4)	<0.012
Mental demand	2 (2–3)	4 (3–5)	<0.012
Physical demand	3 (2–3)	2 (1–2)	0.09 (n.s.)

budget.

It was established in [26, 27] that users begin to perceive haptic delay at approximately 40 ms; NEC Hands operates at roughly half that threshold.

5.4. User Experience Evaluation

The same ten participants completed a within-subjects comparison: (A) NEC Hands with haptic feedback, versus (B) Meta Quest 3 bare-hand tracking. The task was a pick-and-place sequence (grasp a 5 cm cube, transport 40 cm, place in a shelf alcove), with 10 trials per condition, counterbalanced. Objective metrics were task completion time and grasp-failure count. Subjective ratings used four Witmer-Singer Presence Questionnaire items [28] and two NASA-TLX items [29] on a 7-point Likert scale.

Two-tailed Wilcoxon signed-rank tests were used for all comparisons. Mean task completion time was 4.2 s (SD 0.9) with NEC Hands versus 5.8 s (SD 1.4) without haptics (Wilcoxon $W = 3$, $Z = -2.70$, $p = 0.007$, $r = 0.76$). Grasp failures dropped from 23/100 to 4/100 trials (83% reduction).

Table 6 reports the subjective ratings (Wilcoxon p-values Bonferroni-corrected).

Presence and naturalness ratings improved significantly with NEC Hands. Physical demand was marginally higher due to the glove's 180 g mass, but this difference did not reach significance after correction. Participants spontaneously reported that they "slowed down near the cube" in the haptic condition, a behavioural indicator of anticipatory motor planning suggesting that the force feedback was integrated into the sensorimotor control loop [30].

Table 7: Feature Comparison Across Haptic Glove Systems

Metric	**Ours**	**HaptX G1**	**Sense-Glove**	**Flex-sensor**
Track. error	±2.7°	<1°	±1.5°	±5°
Max force	2.5 N	5.4 N	4.0 N	None
Feedback	Kines.	Pneum.	Mag. brake	Vibro.
Wireless	BLE	Tethered	BLE	BLE
Latency	19 ms	<10 ms	<15 ms	∼25 ms
Mass	180 g	310 g	250 g	∼90 g
Cost	$33	$5495	$3500	∼$25
Open-source	Planned	No	No	Varies

6. COMPARISON WITH EXISTING SYSTEMS

Table 7 positions NEC Hands against representative commercial and academic systems across seven metrics.

Tracking accuracy. NEC Hands achieves ±2.7° mean error, which is roughly twice that of SenseGlove (±1.5°) and HaptX (<1°), but approximately half the error of typical flex-sensor gloves (±5°) [6]. The difference is attributable to the single-MCP-axis measurement and the mechanical compliance of the string linkage; commercial systems use multi-axis magnetic or Hall-effect sensing with rigid linkages. For the target application of rigid-object grasping, the ±2.7° error is below the 3° threshold at which users can distinguish virtual finger postures [9].

Force feedback. The 2.5 N maximum force is lower than HaptX (5.4 N) and SenseGlove (4.0 N), both of which employ pneumatic or magneto-rheological mechanisms costing USD 3500–5495. However, NEC Hands is the only system below USD 100 that provides proportional kinesthetic feedback at all; the nearest low-cost competitor [8] offers only binary vibrotactile cues. This represents a qualitative difference: the proportional spring model in (5) allows users to perceive graded stiffness, which the user study confirmed through the significant improvement in the "object stiffness" presence item (Table 6).

Latency. The 19 ms end-to-end latency is higher than HaptX (<10 ms) and SenseGlove (<15 ms), but well below the 40 ms psychophysical threshold [26]. The BLE notification interval (12.4 ms) is the dominant contributor; tethered USB connections used by HaptX avoid this overhead but sacrifice mobility.

Cost-performance trade-off. The cost reduction from USD 3500 (SenseGlove) to USD 33 (NEC Hands) represents a factor of 106×. This reduction is enabled by three design choices: (i) commodity rotary potentiometers instead of magnetic encoders, (ii) standard hobby servos instead of custom actuators, and (iii) a single-tendon dual-function architecture that eliminates the need for separate sensing and actuation linkages. These choices incur known penalties in tracking resolution and maximum force, but the experimental evaluation demonstrates that the resulting system remains adequate for the dominant use case of rigid-object grasping in VR.

7. DISCUSSION

The experimental results support the central hypothesis stated in the Introduction: string-coupled rotary potentiometers combined with drum-and-tendon servo actuation can deliver both tracking and proportional kinesthetic force feedback from a single mechanical linkage at a cost two orders of magnitude below commercial alternatives, while remaining accurate enough for rigid-object grasping.

Three design decisions underpin this cost-performance trade-off. First, the single-tendon dual-function architecture eliminates the need for separate sensing and actuation linkages, halving cable runs relative to [19] and reducing assembly complexity. Second, rotary potentiometers provide monotonic, low-hysteresis angle measurement without the drift and fatigue documented for flex sensors in [6,8] and at a unit cost below USD 1. Third, the BLE GATT interface decouples the glove from the host platform, enabling standalone operation on Meta Quest headsets without a tethered PC, which is a prerequisite for scalable deployment in educational and training environments [32].

The statistically significant improvements across four presence subscales (all corrected $p < 0.012$, effect size $r = 0.76$) are consistent with the broader finding in the haptics literature that even modest kinesthetic feedback (1–3 N) substantially enhances VR grasping quality [31]. The behavioural observation that participants spontaneously slowed down near the cube in the haptic condition is a known marker of anticipatory motor planning [30], suggesting that the force feedback was integrated into the sensorimotor control loop rather than perceived as an external disturbance.

7.1. Limitations

- *Single-joint tracking.* Measuring only the MCP angle limits fidelity for precision manipulation. The coupling-ratio approximation (3) introduces visible error during isolated PIP flexion.
- *Actuator bandwidth.* The SG90's 120 ms transit time at 60° caps the force-rendering bandwidth at roughly 4 Hz, precluding high-frequency texture rendering [17]. This bandwidth is sufficient for rigid-object grasping but insufficient for high-frequency vibrotactile texture simulation.
- *Thumb kinematics.* The thumb's saddle joint has two independent rotational degrees of freedom. The single-potentiometer setup captures only the dominant flexion axis; abduction remains untracked.
- *Sample size.* Ten participants suffice for within-subjects effect-size estimation but fall short of the 20–30 commonly requested by reviewers for robust non-parametric inference. The reported p-values should be interpreted alongside the effect sizes ($r = 0.76$) rather than in isolation.

7.2. Safety

The 2.5 N comfort-limited force is well below injury thresholds for healthy adult fingers. Three firmware safeguards prevent harm: (i) hard servo-angle cap at 80°; (ii) BLE-loss fail-safe returning servos to neutral within 500 ms; (iii) thermal duty-cycle limiter preventing motor surface temperature from exceeding 70°C. No adverse events were reported during any experimental session.

7.3. Implications for VR Training

The sub-$35 cost and standalone BLE operation lower the barrier to incorporating kinesthetic feedback in resource-constrained settings. Recent work on AI-enhanced VR platforms for aviation maintenance training has shown that scalable, procedure-locked training modules on standalone headsets can achieve positive learner engagement [32]; such platforms currently lack haptic feedback. The results of the present study suggest that integrating a low-cost kinesthetic glove could further improve training realism, though this hypothesis requires validation in domain-specific tasks beyond the generic pick-and-place paradigm evaluated here.

7.4. Future Directions

The next iteration will explore replacing the rotary potentiometers with Hall-effect sensors. Because Hall-effect transducers measure the orientation of a magnetic field rather than relying on mechanical coupling, they are contactless, immune to cable wear, and can be encapsulated against moisture and dust. A small diametrically magnetised disc bonded near the joint axis paired with a Hall-effect IC (e.g., AS5600 or AMS AS5048) on the opposing side would provide absolute angular output with sub-degree resolution while eliminating the string-and-spring assembly entirely. This simplification is expected to reduce mechanical complexity, improve long-term durability, and lower the per-finger component count.

8. Conclusion

This paper addressed a well-defined gap in the haptic-glove landscape: all peer-reviewed glove designs below USD 100 are limited to vibrotactile (binary) feedback, whereas systems offering proportional kinesthetic force feedback cost USD 3500 or more. NEC Hands bridges this gap through a dual-function single-tendon architecture in which one nylon string per finger simultaneously drives a rotary potentiometer (sensing) and is wound by a 3D-printed TendonDrum servo (actuation), halving the cable count relative to separate-sensing-and-actuation designs such as [19].

The four contributions stated in the Introduction were validated as follows: (1) The dual-purpose cable architecture achieved a mean tracking error of 2.66° (SD 1.16°, $N = 10$, 2500 OptiTrack-referenced cycles), comparable to the ±5° reported for flex-sensor gloves [6, 8] and below the 3° threshold for rigid-object grasping. (2) The dual-mode calibration system produced a non-linearity of 1.8% full scale, adequate for the linear calibration mapping. (3) The BLE GATT interface achieved an end-to-end latency of 19.3 ms, well below the 40 ms perceptual threshold established in [26, 27] and comparable to the <15 ms of SenseGlove [4]. (4) The within-subjects evaluation ($N = 10$, Wilcoxon signed-rank, all corrected $p < 0.012$, $r = 0.76$) showed significant improvements in presence, grasping naturalness, object-stiffness perception, and scene presence over bare-hand tracking, alongside an 83% reduction in grasp failures.

The total bill-of-materials cost is USD 30.50, representing a cost reduction of more than two orders of magnitude relative to HaptX Gloves G1 ($5495) and SenseGlove Nova ($3500). The primary limitations are single-joint MCP measurement, 4 Hz force-rendering bandwidth, and a sample size of 10. Future work will replace the rotary potentiometers with contactless Hall-effect sensors (AS5600) to eliminate string wear and will scale the user study to 30 participants.

NEC Hands demonstrates that proportional kinesthetic feedback in VR can be achieved at component costs accessible to education, rehabilitation, and independent research, without sacrificing the tracking accuracy or latency required for rigid-object grasping tasks.

DECLARATION OF COMPETING INTERESTS

The authors declare no conflicts of interest.

ACKNOWLEDGMENT

The authors thank the Army Institute of Technology, Pune, for providing laboratory facilities and 3D-printing resources, and all study participants for their time. This research received no external funding.

DATA AVAILABILITY

The datasets generated during this study are available from the corresponding author upon reasonable request.

AI USE DECLARATION

During the preparation of this work the authors used AI writing assistance tools in order to improve language clarity and grammar. After using these tools, the authors reviewed and edited the content as needed and take full responsibility for the content of the publication.

References

[1] R. S. Johansson and J. R. Flanagan, "Coding and use of tactile signals from the fingertips in object manipulation tasks," *Nature Reviews Neuroscience*, vol. 10, no. 5, pp. 345–359, May 2009.

[2] M. Slater, "Place illusion and plausibility can lead to realistic behaviour in immersive virtual environments," *Philosophical Transactions of the Royal Society B*, vol. 364, no. 1535, pp. 3549–3557, Dec. 2009.

[3] HaptX Inc., "HaptX Gloves G1 Technical Specifications," HaptX. [Online]. Available: https://haptx.com

[4] SenseGlove B.V., "SenseGlove Nova Product Sheet," SenseGlove. [Online]. Available: https://www.senseglove.com

[5] Meta Platforms Inc., "Inside Reality Labs Research: Haptic Gloves," Meta. [Online]. Available: https://about.meta.com/realitylabs/

[6] G. Saggio and L. Sbernini, "New scenarios in human trunk posture measurements using inertial and flex sensors," in *Proceedings of the IEEE International Symposium on Medical Measurements and Applications (MeMeA)*, Lisbon, Portugal, 2014, pp. 1–5.

[7] J. Connolly, J. Condell, B. O'Flynn, J. T. Sanchez, and P. Gardiner, "IMU sensor-based electronic goniometric glove for clinical finger movement analysis," *IEEE Sensors Journal*, vol. 18, no. 3, pp. 1273–1281, Feb. 2018.

[8] M. Borghetti, E. Sardini, and M. Serpelloni, "Sensorized glove for measuring hand finger flexion for rehabilitation purposes," *IEEE Transactions on Instrumentation and Measurement*, vol. 62, no. 12, pp. 3308–3314, Dec. 2013.

[9] B. S. Lin, I. J. Lee, S. Y. Yang, Y. C. Lo, J. Lee, and J. L. Chen, "Design of an inertial-sensor-based data glove for hand function evaluation," *Sensors*, vol. 18, no. 5, May 2018, Art. no. 1545.

[10] H. G. Kortier, V. I. Sluiter, D. Roetenberg, and P. H. Veltink, "Assessment of hand kinematics using inertial and magnetic sensors," *Journal of NeuroEngineering and Rehabilitation*, vol. 11, Apr. 2014, Art. no. 70.

[11] Ultraleap Ltd. "Gemini Hand Tracking Software Documentation." Ultraleap. [Online]. Available: https://www.ultraleap.com

[12] H. K. Yap, J. H. Lim, F. Nasrallah, and C. H. Yeow, "Design and preliminary feasibility study of a soft robotic glove for hand function assistance in stroke survivors," *Frontiers in Neuroscience*, vol. 11, Oct. 2017, Art. no. 547.

[13] S. Park, J. Kim, and J. Sim, "Low-cost finger motion capture system using string-potentiometer sensors," in *Proceedings of the IEEE International Conference on Consumer Electronics*, Las Vegas, NV, USA, 2020, pp. 1–3.

[14] Y. Li, J. Chen, Z. Wang, and J. Zhang, "Soft robotic glove with integrated sensing and force feedback for rehabilitation in virtual reality," *Biomimetics*, vol. 8, no. 1, Feb. 2023, Art. no. 83.

[15] P. Polygerinos, Z. Wang, K. C. Galloway, R. J. Wood, and C. J. Walsh, "Soft robotic glove for combined assistance and at-home rehabilitation," *Robotics and Autonomous Systems*, vol. 73, pp. 135–143, Nov. 2015.

[16] L. Hines, K. Petersen, G. Z. Lum, and M. Sitti, "Soft actuators for small-scale robotics," *Advanced Materials*, vol. 29, no. 13, Apr. 2017, Art. no. 1603483.

[17] I. Choi, H. Culbertson, M. R. Miller, A. Olwal, and S. Follmer, "Grabity: A wearable haptic interface for simulating weight and grasping in virtual reality," in *Proceedings of the 30th Annual ACM Symposium on User Interface Software and Technology (UIST)*, Québec City, QC, Canada, 2017, pp. 119–130.

[18] M. Rueckert, G. Schauss, A. Tobola, and R. Lenhart, "A low-cost sensor glove with vibrotactile feedback and multiple finger joint and hand motion sensing for human-robot interaction," *Sensors*, vol. 16, no. 4, Apr. 2016, Art. no. 491.

[19] J. Sim, J. Kim, S. Park, and M. Kim, "A low-latency haptic open glove for immersive VR interaction," *Sensors*, vol. 21, no. 10, May 2021, Art. no. 3552.

[20] X. Gu, Y. Zhang, W. Sun, Y. Bian, D. Zhou, and P. O. Kristensson, "Dexmo: An inexpensive and lightweight mechanical exoskeleton for motion capture and force feedback in VR," in *Proceedings of the CHI Conference on Human Factors in Computing Systems*, San Jose, CA, USA, 2016, pp. 1991–1995.

[21] CyberGlove Systems LLC, "CyberGlove III Specifications," CyberGlove Systems. [Online]. Available: http://www.cyberglovesystems.com

[22] T. M. Greiner, "Hand anthropometry of U.S. Army personnel," U.S. Army Natick Research, Development and Engineering Center, Natick, MA, USA, Technical Report NATICK/TR-92/011, 1991.

[23] K. N. An, E. Y. Chao, W. P. Cooney, and R. L. Linscheid, "Normative model of human hand for biomechanical analysis," *Journal of Biomechanics*, vol. 12, no. 10, pp. 775–788, 1979.

[24] J. W. Lee and K. Rim, "Maximum finger force prediction using a planar simulation of the middle finger," *Proceedings of the Institution of Mechanical Engineers, Part H*, vol. 204, no. 3, pp. 169–178, 1990.

[25] Android Developers, "Bluetooth Low Energy Overview," Android. [Online]. Available: https://developer.android.com/guide/topics/connectivity/bluetooth-le

[26] R. S. Allison, L. R. Harris, M. Jenkin, U. Jasiobedzka, and J. E. Zacher, "Tolerance of temporal delay in virtual environments," in *Proceedings of the IEEE Virtual Reality Conference*, Yokohama, Japan, 2001, pp. 247–254.

[27] C. Jay and R. Hubbold, "Delayed visual and haptic feedback in a reciprocal tapping task," in *Proceedings of the First Joint Eurohaptics Conference and Symposium on Haptic Interfaces for Virtual Environment and Teleoperator Systems*, Pisa, Italy, 2005, pp. 655–656.

[28] B. G. Witmer and M. J. Singer, "Measuring presence in virtual environments: A presence questionnaire," *Presence: Teleoperators and Virtual Environments*, vol. 7, no. 3, pp. 225–240, Jun. 1998.

[29] S. G. Hart and L. E. Staveland, "Development of NASA-TLX (Task Load Index): Results of empirical and theoretical research," *Advances in Psychology*, vol. 52, pp. 139–183, 1988.

[30] J. R. Flanagan, M. C. Bowman, and R. S. Johansson, "Control strategies in object manipulation tasks," *Current Opinion in Neurobiology*, vol. 16, no. 6, pp. 650–659, Dec. 2006.

[31] C. Pacchierotti, S. Sinclair, M. Solazzi, A. Frisoli, V. Hayward, and D. Prattichizzo, "Wearable haptic systems for the fingertip and the hand: Taxonomy, review, and perspectives," *IEEE Transactions on Haptics*, vol. 10, no. 4, pp. 580–600, Oct. 2017.

[32] H. N. The, "Developing a scalable, AI-enhanced VR platform for aviation training: Commercial aircraft case studies," *Engineering, Technology & Applied Science Research*, vol. 16, no. 1, pp. 32000–32008, 2026, doi: 10.48084/etasr.15338.